



NUMERICAL SIMULATION AND ANALYSIS OF THE MODIFIED BURGERS' EQUATION IN DUSTY PLASMAS

 Harekrishna Deka^a,  Jnanjyoti Sarma^b

^a*K.K. Handiqui State Open University, Khanapara, Guwahati, 781022, India*

^b*R.G. Baruah College, Fatasil Ambari, Guwahati, 781025, India*

* *Corresponding Author e-mail: harekrishnadeka11@gmail.com*

Received July 30, 2023; revised September 16, 2023; accepted September 25, 2023

This paper presents a comprehensive study on the numerical simulation of the one-dimensional modified Burgers' equation in dusty plasmas. The reductive perturbation method is employed to derive the equation, and a numerical solution is obtained using the explicit finite difference technique. The obtained results are extensively compared with analytical solutions, demonstrating a high level of agreement, particularly for lower values of the dissipation coefficient. The accuracy and efficiency of the technique are evaluated based on the absolute error. Additionally, the accuracy and effectiveness of the technique are assessed by plotting L_2 and L_∞ error graphs. The technique's reliability is further confirmed through von-Neumann stability analysis, which indicates that the technique is conditionally stable. Overall, the study concludes that the proposed technique is successful and dependable for numerically simulating the modified Burgers' equation in dusty plasmas.

Keywords: *Dusty plasmas; Reductive perturbation method; Modified Burgers equation; Finite difference explicit technique; von Neumann stability analysis*

PACS: 02.70Bf, 52.27Lw, 52.35Fp, 52.35Tc

1. INTRODUCTION

Wave propagation in dusty plasmas [1] has gained significant attention in recent years due to its relevance in astrophysical and space environments, as well as in the lower ionosphere of the Earth [2, 3, 4, 5, 6]. The presence of charged dust particles in dusty plasmas has a notable impact on the spectra of normal plasma waves [7], giving rise to the emergence of two kind of low-frequency waves [8] in dusty plasmas, including dust acoustic waves [9, 10] and dust-ion-acoustic waves [8, 9]. Dust-acoustic waves (DAWs) have numerous industrial uses, including in laboratory plasma equipment, semiconductor chip manufacturing, and fusion reactor systems [11, 12]. Numerous researchers have investigated the characteristics of nonlinear wave propagation in dusty plasmas. Tamang and Saha [13] presented dynamic transitions of dust acoustic waves in collisional dusty plasmas. Dev et al. [14] have derived the n th-order three-dimensional modified Burgers' equation, considering non-thermal ions with varying temperatures. Tian et al. [15] analyzed a new $(3 + 1)$ -dimensional modified Burgers' equation with the electron distribution in the presence of trapping particles and the kinetic equation of charge of dust particle. This paper investigates the one-dimensional modified Burgers' equation in a dusty plasma medium. The MBE has the strong non-linear behaviours and also has widely been utilized in physical phenomena [16]. The MBE equation is a nonlinear advection-diffusion equation [17]. The primary objective is to numerically solve the equation and explore the diverse characteristics of shock waves. Numerous authors in the literature have suggested and applied diverse numerical techniques to approximate the solution of the modified Burgers' equation. A summary of the suggested numerical techniques for approximating the solution of the modified Burgers' equation includes the following:

Zeytinoglu et al. [18] investigated an efficient numerical method for analyzing the propagation of shock waves in the equation. Bratsos [19] employed a finite difference technique as a computational method to solve the equation. Ramadan et al. [20] employed a septic B-spline collocation approach for solving the equation. Irk [21] have applied the sextic B-spline collocation technique for solving the equation. Saka and Dag [22] used quintic B-splines collocation technique to solve the equation. Duan et al. [23] implemented Lattice Boltzmann method to solve the equation. A Chebyshev spectral collocation method is applied by Temsah [24]. Roshan and Sharma [25] applied the Petrov-Galerkin method for solving the equation. Kutluay et al. [26] implemented a cubic B-spline collocation technique for solving the equation. Also, Ucar et al. [27] used finite difference technique for solving the equation. Gao et al. [28] developed a high bounded upwind scheme within the normalized-variable formulation to approximate the equation. Grienwank et al. [29] introduced a non-polynomial spline-based method for solving the equation. Bratsos et al. [30] employed the explicit finite difference scheme to numerically solve the equation. Numerical solution of nonlinear modified Burgers' equation

is obtained using an improvised collocation technique with cubic B-spline as basis functions in [31]. The authors in [32] provided an orthogonal collocation technique with septic Hermite splines as basis function to obtain the numerical solution of non-linear modified Burgers' equation. A numerical method based on quintic trigonometric B-splines for solving modified Burgers' equation (MBE) is presented in [33]. The arrangement of the manuscript is as follows. Section 2 of the manuscript discusses the governing equations of the dusty plasma model, along with the derivation of the modified Burgers' equation in dusty plasmas. Section 3 presents the explicit finite difference technique. The stability analysis of this technique is presented in Section 4. Section 5 includes the results and discussion, while the conclusion is provided in Section 6.

2. GOVERNING EQUATIONS AND DERIVATION OF MODIFIED BURGERS' EQUATION

The governing equations for the dusty plasma model are:

$$\frac{\partial n_d}{\partial t} + \nabla \cdot (n_d u_d) = 0 \tag{1}$$

$$\frac{\partial u_d}{\partial t} + (u_d \cdot \nabla) u_d = \frac{Z_d e}{m_d} \nabla \Psi - \frac{\nabla p_d}{m_d n_d} \tag{2}$$

The Poisson equation is expressed as follows

$$\nabla^2 \Psi = 4\pi e [n_e + Z_d n_d - n_{il} - n_{ih}] \tag{3}$$

where u_d represents the fluid speed, Z_d denotes the dust charge number, m_d represents the mass of the dust particle, Ψ represents the electrostatic potential, and n_d represents the dust particle number density. Additionally, n_{il} represents the ion particle number density at lower temperature, n_{ih} represents the ion particle number density at higher temperature, and n_e represents the electron particle number density.

The electron density, as well as the ion densities at both low and high temperatures, are provided as follows:

$$n_e = \left(\frac{1}{\sigma_1 + \sigma_2 - 1} \right) e^{\left(\frac{s\theta_1 \Psi}{\kappa_B T_e} \right)} \tag{4}$$

$$n_{il} = \left(\frac{\sigma_1}{\sigma_1 + \sigma_2 - 1} \right) \left(1 + \eta g \varphi + \eta (g \varphi)^2 \right) \exp \left(\frac{-g \Psi}{\kappa_B T_{il}} \right) \tag{5}$$

$$n_{ih} = \left(\frac{\sigma_1}{\sigma_1 + \sigma_2 - 1} \right) \left(1 + \eta g \rho \varphi + \eta (g \theta \varphi)^2 \right) \exp \left(\frac{-g \rho \Psi}{\kappa_B T_{ih}} \right) \tag{6}$$

where $\theta_1 = \frac{T_{il}}{T_e}$, $\theta_2 = \frac{T_{ih}}{T_e}$, $\theta = \frac{\theta_1}{\theta_2} = \frac{T_{il}}{T_{ih}}$, $\sigma_1 = \frac{n_{il0}}{n_{e0}}$, $\sigma_2 = \frac{n_{ih0}}{n_{e0}}$, $g = \frac{T_{eff}}{T_{il}} = \frac{\sigma_1 + \sigma_2 - 1}{\sigma_1 + \sigma_2 \theta + \theta_1}$, $\varphi = \frac{e \Psi}{\kappa_B T_{eff}}$ and $\eta = \frac{4\kappa}{1+3\kappa}$.

The charge equation is written as [35, 36]

$$\frac{d\bar{Q}_d}{dt} + \nu \bar{Q}_d = |I_{e0}| n_{d0} Z_{d0} \left(\frac{\bar{n}_{il}}{n_{il0}} + \frac{\bar{n}_{ih}}{n_{ih0}} - \frac{\bar{n}_e}{n_{e0}} \right) \tag{7}$$

with $Q_d = \bar{Q}_d + Q_{d0}$ where \bar{Q}_d and Q_{d0} are the charged of the dust particle at perturbed and equilibrium states respectively. The natural decay rate ν is defined as $\nu = \frac{e|I_{e0}|}{C} \left[\frac{1}{\kappa_B T_{eff}} + \frac{1}{\aleph_0} \right]$ and $\aleph_0 = \kappa_B T_{eff} - e \Psi_{f0}$, with Ψ_{f0} is the floating potential at equilibrium.

The effective temperatures T_{eff} for two types of ions, namely, ions at low temperature and ions at high temperature, are provided.

$$T_{eff} = \left[\frac{1}{n_{d0} Z_{d0}} \left(\frac{n_{e0}}{T_e} + \frac{n_{il0}}{T_{il}} + \frac{n_{ih0}}{T_{ih}} \right) \right]^{-1} \tag{8}$$

The equations 1, 2, 3 and 7 can be expressed in their normalized form as follows:

$$\frac{\partial N_d}{\partial T} + \nabla \cdot (N_d U_d) = 0 \tag{9}$$

$$\left(\frac{\partial}{\partial T} + U_d \nabla \right) U_d = Z_d \nabla \psi - \Omega \frac{5}{3} N_d^{-1} \nabla N_d^\xi \tag{10}$$

$$\nabla^2\psi = \Upsilon_1\psi + \Upsilon_2\psi^2 + (Z_d N_d - 1) \tag{11}$$

$$\frac{dZ_d}{dt} + \nu' Z_d = r + r_1\psi + r_2\psi^2 \tag{12}$$

where $\Upsilon_1 = \frac{\theta_1 + (\sigma_1 + \sigma_2\theta)(1-\eta)}{\sigma_1 + \sigma_2 - 1}g$, $\Upsilon_2 = \frac{\theta_1^2 - \sigma_1 - \sigma_2\theta^2}{2(\sigma_1 + \sigma_2 - 1)}g^2$, $\Omega = \frac{T_d}{T_{eff}}$, $r = \frac{|I_{e0}|}{ez_{d0}\omega_{pd}}$, $r_1 = \frac{|I_{e0}|[(\eta-1)(1+\theta) - \theta_1]}{ez_{d0}\omega_{pd}}$, $r_2 = \frac{|I_{e0}|(1+\theta^2 - \theta_1^2)}{2ez_{d0}\omega_{pd}}g^2$, $\nu' = \frac{\nu}{\omega_{pd}}$ and N_d is the number density of dust particle and is normalized by n_{d0} , U_d is the fluid velocity which is normalized by $c_d = \sqrt{\frac{Z_{d0}k_B T_{eff}}{m_d}}$, ψ is the electrostatic potential which is normalized by $\psi = \frac{e\Psi}{K_B T_{eff}}$ and charge density Z_d is normalized by Z_{d0} . x is normalized by the dust $\lambda_D = \left(\frac{K_B T_{eff}}{4\pi n_{d0} e^2 Z_{d0}}\right)^{\frac{1}{2}}$ and time variable t is normalized by the dust plasma frequency $\omega_{pd} = \left(\frac{4\pi Z_{d0}^2 n_{d0} e^2}{m_d}\right)^{\frac{1}{2}}$. The adiabatic index $\xi = 3$ for the one dimensional geometry of the system.

For employing reductive perturbation theory, the space and time stretched coordinates are as follows:

$$\zeta = \epsilon^3 (x - V_p t); \tau = \epsilon^6 t \tag{13}$$

where ϵ represents a small quantity that characterizes the nonlinearity in the system, and V_p is the phase speed of the wave. The variables N_d , Z_d , ψ and U_{dx} are expanded as power series in terms of ϵ as shown below:

$$N_d = 1 + \epsilon N_d^{(1)} + \epsilon^2 N_d^{(2)} + \epsilon^3 N_d^{(3)} + \dots \tag{14}$$

$$Z_d = 1 + \epsilon Z_d^{(1)} + \epsilon^2 Z_d^{(2)} + \epsilon^3 Z_d^{(3)} + \dots \tag{15}$$

$$\psi = \epsilon\psi^{(1)} + \epsilon^2\psi^{(2)} + \epsilon^3\psi^{(3)} + \dots \tag{16}$$

$$U_{dx} = \epsilon U_{dx}^{(1)} + \epsilon^2 U_{dx}^{(2)} + \epsilon^3 U_{dx}^{(3)} + \dots \tag{17}$$

After substituting the relations 13-17 into equations 9-12 and performing some algebraic manipulations, the following equation has been obtained [14] as:

$$\frac{\partial\psi^{(1)}}{\partial\tau} + A [\psi^{(1)}]^3 \frac{\partial\psi^{(1)}}{\partial\zeta} = B \frac{\partial^2\psi^{(1)}}{\partial\zeta^2} \tag{18}$$

The nonlinear coefficient A is given in the form

$$A = \frac{e^2 z_{d0} (z_{d0} + r_1)}{V_p^3 m_d^2} - \frac{e^2 r_1 z_{d0}}{V_p^3 m_d^2 \theta} - \frac{4}{3} \frac{er_2}{m_d V_p} + \frac{e^3 (z_{d0})^3}{4V_p^5 m_d^3} - \frac{r_1^2 e}{4m_d V_p z_d^{(0)} \theta^2} + \frac{r_2 e^2}{V_p m_d \theta} - \frac{e}{2m_d V_p z_{d0} \theta^2} + \frac{r_1 r_2 V_p}{4\theta^2 (z_{d0})^2} + \frac{r_1^2 V_p}{16\theta^3 (z_{d0})^2} \tag{19}$$

and the dissipation coefficient B is represented by

$$B = \frac{V_p^4 r}{2\omega_{pd}^2 \theta^2} \tag{20}$$

The equation 18 is commonly referred to as the one-dimensional modified Burgers' equation in dusty plasmas. It serves as a fundamental model for describing various phenomena, including shock wave solutions, mass transport, gas dynamics in plasma, and fluid dynamics.

The travelling wave solution [14] of 18 is derived as

$$\psi^{(1)} = \left\{ \psi_m \left[1 - \tanh\left(\frac{\nu}{\delta}\right) \right] \right\}^{\frac{1}{3}} \tag{21}$$

Here, $\psi_m = \frac{4Vl}{2Al^2} = \frac{2V}{Al}$ represents the amplitude of the shock wave, and $\delta = \frac{2Bl^3}{Vl} = \frac{2Bl^2}{V}$ represents its width. In these equations, l denotes the direction cosines, and V is the speed of the shock wave. Substituting $v = \zeta l - V\iota$, $\psi_m = \frac{2V}{Al}$ and $\delta = \frac{2Bl^2}{V}$ in 21, the travelling wave solution of modified Burgers' equation becomes

$$\psi^{(1)}(\zeta, \iota) = \left\{ \frac{2V}{Al} \left[1 - \tanh \left(\frac{\zeta l - V\iota}{\frac{2Bl^2}{V}} \right) \right] \right\}^{\frac{1}{3}} \tag{22}$$

3. EXPLICIT FINITE DIFFERENCE METHOD

For convenience, we consider $\psi^{(1)}(\zeta, \iota) = u(x, t)$ and $l = 1$. The equation 18 is rewritten as

$$\frac{\partial u}{\partial t} + Au^3 \frac{\partial u}{\partial x} = B \frac{\partial^2 u}{\partial x^2} \tag{23}$$

The travelling wave solution of equation is written by

$$u(x, t) = \left\{ \frac{2V}{A} \left[1 - \tanh \frac{V}{4B} \left(x - \frac{t}{2} \right) \right] \right\}^{\frac{1}{3}} \tag{24}$$

with the initial condition,

$$u(x, 0) = \left\{ \frac{2V}{A} \left[1 - \tanh \left(\frac{Vx}{4B} \right) \right] \right\}^{\frac{1}{3}} \tag{25}$$

and the boundary conditions

$$u(0, t) = \left\{ \frac{2V}{A} \left(1 + \tanh \frac{Vt}{8B} \right) \right\}^{\frac{1}{3}} \tag{26}$$

$$u(1, t) = \left\{ \frac{2V}{A} \left[1 - \tanh \frac{V}{4B} \left(1 - \frac{t}{2} \right) \right] \right\}^{\frac{1}{3}} \tag{27}$$

In order to discretize the modified Burgers' equation 23, we apply the forward difference approximation to replace the partial derivative $\frac{\partial u}{\partial t}$ and the central difference approximation to replace the partial derivatives $\frac{\partial u}{\partial x}$ and $\frac{\partial^2 u}{\partial x^2}$, as described in reference[34], i.e.

$$\frac{\partial u}{\partial t} \approx \frac{u_{i,j+1} - u_{i,j}}{k} \tag{28}$$

$$\frac{\partial^2 u}{\partial x^2} \approx \frac{u_{i+1,j} - 2u_{i,j} + u_{i-1,j}}{h^2} \tag{29}$$

$$\frac{\partial u}{\partial x} \approx \frac{u_{i+1,j} - u_{i-1,j}}{2h} \tag{30}$$

thus 23 becomes

$$\frac{u_{i,j+1} - u_{i,j}}{k} + Au_{i,j}^3 \left[\frac{u_{i+1,j} - u_{i-1,j}}{2h} \right] = B \left[\frac{u_{i+1,j} - u_{i,j} + u_{i-1,j}}{h^2} \right] \tag{31}$$

which simplifies

$$u_{i,j+1} = u_{i,j} + \frac{kA}{2h} u_{i,j}^3 [u_{i-1,j} - u_{i+1,j}] + \frac{kB}{h^2} [u_{i+1,j} - 2u_{i,j} + u_{i-1,j}] \tag{32}$$

4. STABILITY ANALYSIS OF THE EXPLICIT FINITE DIFFERENCE METHOD

The von Neumann analysis method is employed to assess the stability of a numerical approach for both linear initial value problems and linearized nonlinear boundary value problems [37]. The Von Neumann stability theory in which the growth factor ξ is defined as

$$u_{i,j} = \xi^j e^{Ikh_i} = \xi^j e^{I\theta i} \tag{33}$$

where $I = \sqrt{-1}$, ξ^j is the amplitude at time level k and $h = \Delta x$. The equation 32 has been linearized by putting $u^3 = M$ to check the stability.

$$u_{i,j+1} = u_{i,j} + \frac{kAM}{2h} [u_{i-1,j} - u_{i+1,j}] + \frac{kB}{h^2} [u_{i+1,j} - 2u_{i,j} + u_{i-1,j}] \tag{34}$$

$$u_{i,j+1} = \left(1 - \frac{2kB}{h^2}\right)u_{i,j} + \left(\frac{kAM}{2h} + \frac{kB}{h^2}\right)u_{i-1,j} + \left(\frac{kB}{h^2} - \frac{kAM}{2h}\right)u_{i+1,j} \tag{35}$$

Substitute 33 in 35, we get

$$\xi^j e^{I\theta i} \xi = \xi^j e^{I\theta i} \left[\left(1 - \frac{2kB}{h^2}\right) + \left(\frac{kAM}{2h} + \frac{kB}{h^2}\right) e^{-I\theta} + \left(\frac{kB}{h^2} - \frac{kAM}{2h}\right) e^{I\theta} \right]$$

$$\xi = \left(1 - \frac{2kB}{h^2}\right) + \left(\frac{kAM}{2h} + \frac{kB}{h^2}\right) e^{-I\theta} + \left(\frac{kB}{h^2} - \frac{kAM}{2h}\right) e^{I\theta}$$

$$\xi = \left(1 - \frac{2kB}{h^2}\right) + \frac{kAM}{2h} (e^{-I\theta} - e^{I\theta}) + \frac{kB}{h^2} (e^{I\theta} + e^{-I\theta})$$

$$\xi = \left(1 - \frac{2kB}{h^2}\right) + \frac{kAM}{2h} (-2I \sin\theta) + \frac{kB}{h^2} (2\cos\theta)$$

$$\xi = \left(1 - \frac{2kB}{h^2}\right) - \frac{kAM}{h} \sin\theta + \frac{2kB}{h^2} \cos\theta$$

The stability criteria for the numerical technique is $|\xi| \leq 1$, which means $-1 \leq \xi \leq 1$ where

$$|\xi| = \left| \left(1 - \frac{2kB}{h^2}\right) - \frac{kAM}{h} \sin\theta + \frac{2kB}{h^2} \cos\theta \right| \leq 1 \tag{36}$$

So the stability condition is $\frac{2kB}{h^2} \leq 1$ or $\frac{kB}{h^2} \leq \frac{1}{2}$

$$k \leq \frac{h^2}{2B} \tag{37}$$

5. RESULTS AND DISCUSSION

Upon evaluating the von Neumann stability condition, we explore different values of B (specifically, $B = 0.001, 0.005, 0.01, 0.05, 0.1, 0.5$) for given step sizes $h = 0.001, 0.01$ and $k = 0.01, 0.05, 0.0001, 0.0005$. The coefficient A is influenced by various plasma parameters, and within these parameters, we consider a specific range of A values, namely $A = 0.2$ to $A = 4$. The validity of the present technique is evaluated using the absolute error which is defined by

$$\left| u_i^{Analytical} - u_i^{Numerical} \right| \tag{38}$$

Also, L_2 and L_∞ error norms, defined by

$$L_2 = \sqrt{h \sum_{j=1}^N \left| u_j^{analytical} - u_j^{numerical} \right|^2} \tag{39}$$

$$L_\infty = \max \left| u_j^{analytical} - u_j^{numerical} \right| \tag{40}$$

are presented graphically for various values of nonlinear coefficient and dissipation coefficient for chosen space and time steps to check the accuracy and effectiveness of the method.

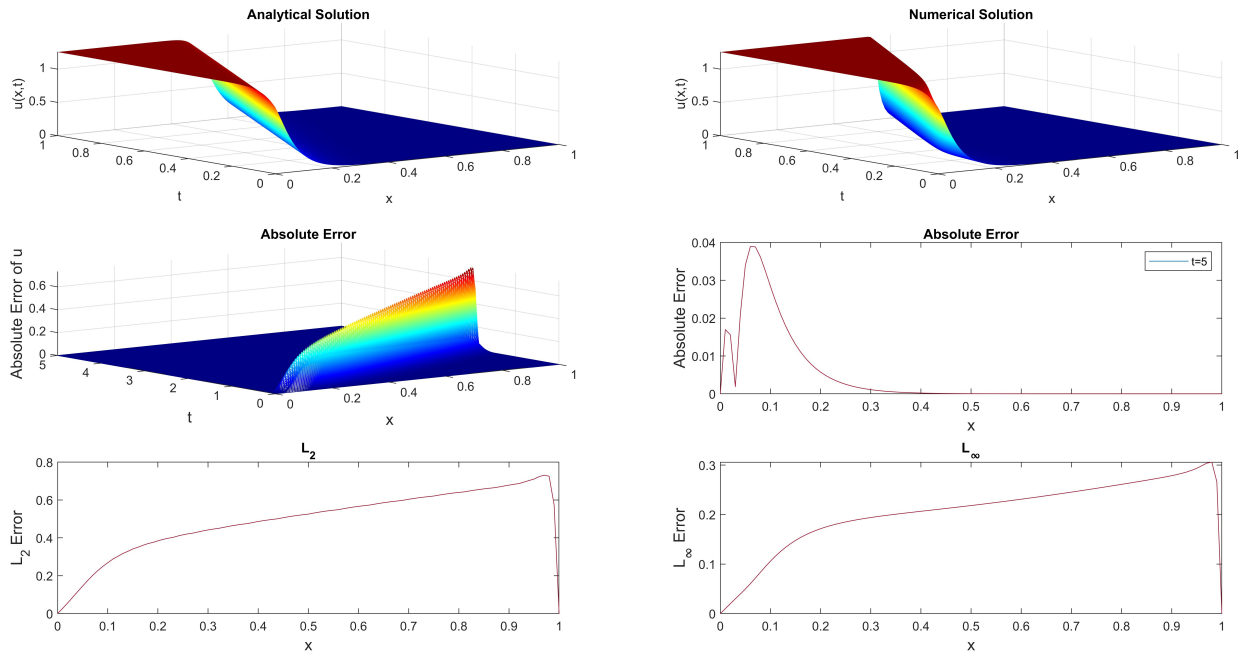


Figure 1. Analytical and numerical solutions, as well as the absolute error, L_2 error norm, and L_∞ error norm, at $A = 1, B = 0.01, h = 0.01,$ and $k = 0.005$.

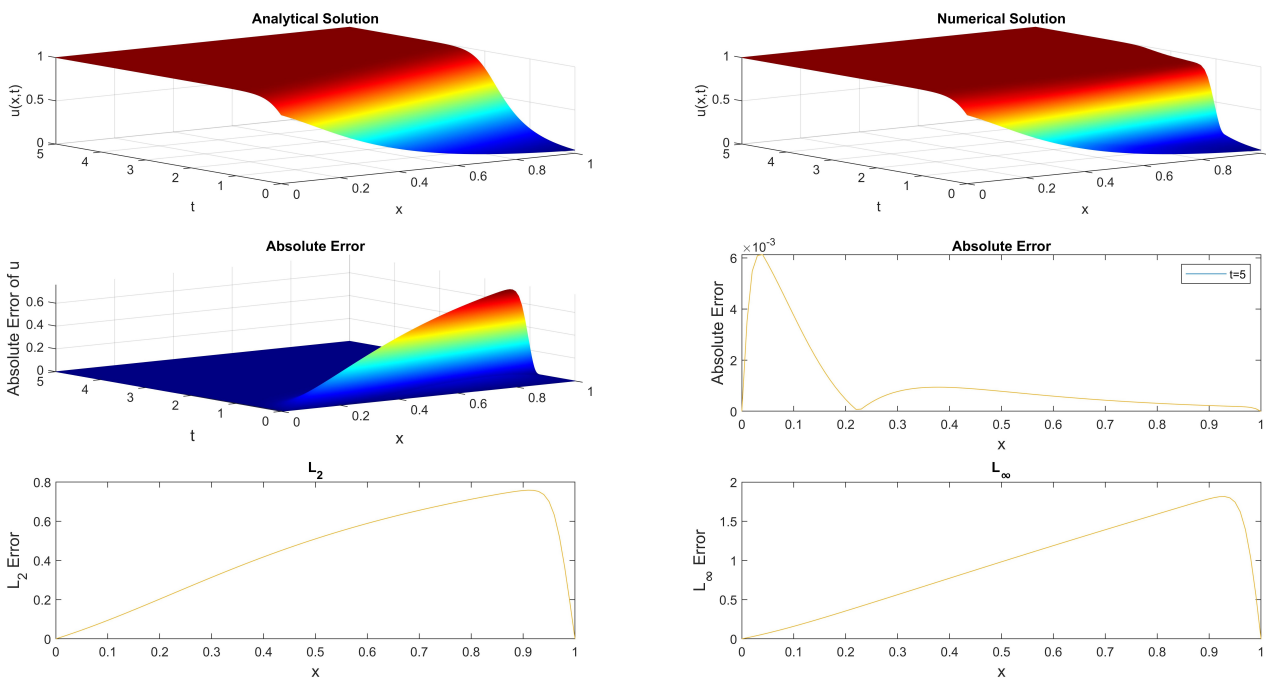


Figure 2. Analytical and numerical solutions, as well as the absolute error, L_2 error norm, and L_∞ error norm, at $A = 2, B = 0.05, h = 0.01, k = 0.001$.

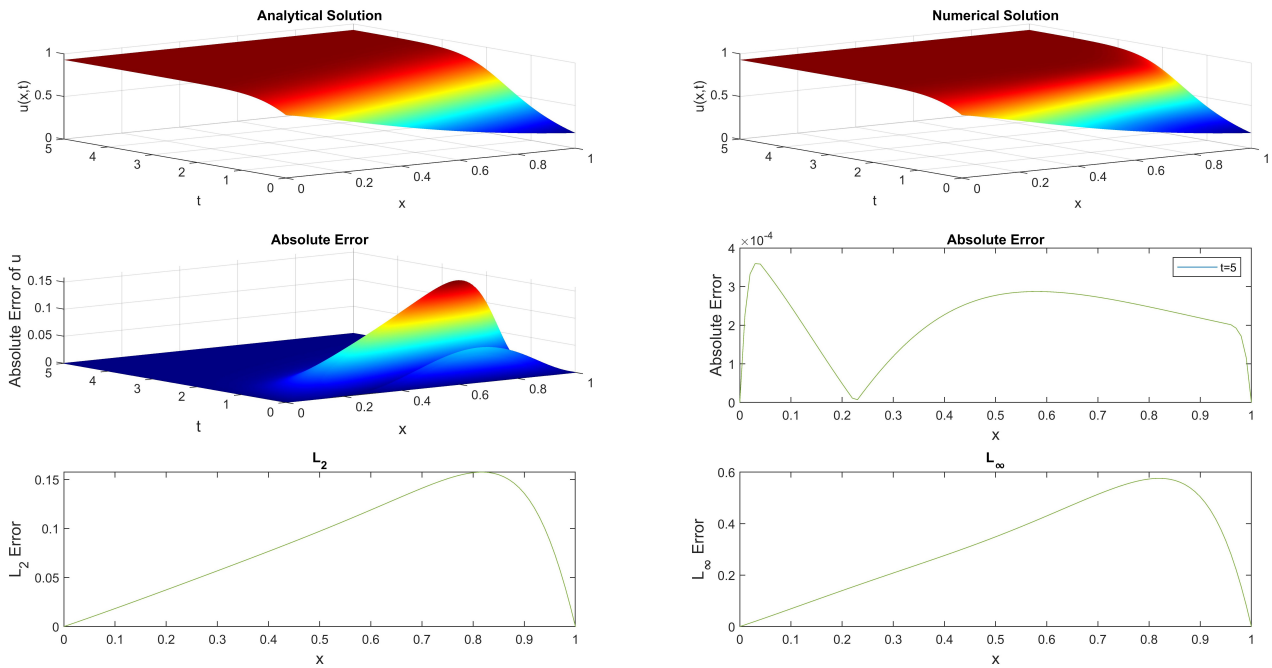


Figure 3. Analytical and numerical solutions, as well as the absolute error, L_2 error norm, and L_∞ error norm, at $A = 2.5, B = 0.1, h = 0.1, k = 0.0005$.

Figures 1-3 demonstrate that the greatest absolute error is observed on the left side of the solution domain for $B = 0.01$ and $B = 0.05$. This suggests that there is a significant discrepancy between the numerical and analytical solutions in that region for these specific values of B . Conversely, the highest error for both the L_2 and L_∞ norms is found on the right side of the solution domain, again for $B = 0.01$ and $B = 0.05$. This implies that the overall accuracy of the numerical solution deteriorates more prominently towards the right side for these particular values of B . Furthermore, by examining Figures 1-3, it can be concluded that as the dissipation coefficient decreases, the wave curves exhibit interesting behavior. Specifically, they become progressively flatter and steeper. This observation suggests that reducing the dissipation coefficient has a noticeable impact on the shape and steepness of the wave curves, indicating a stronger influence of convection effects in the system. Therefore, it can be concluded from the analysis of Figures 1-3 that the dissipation coefficient plays a crucial role in shaping the behavior of the wave curves.

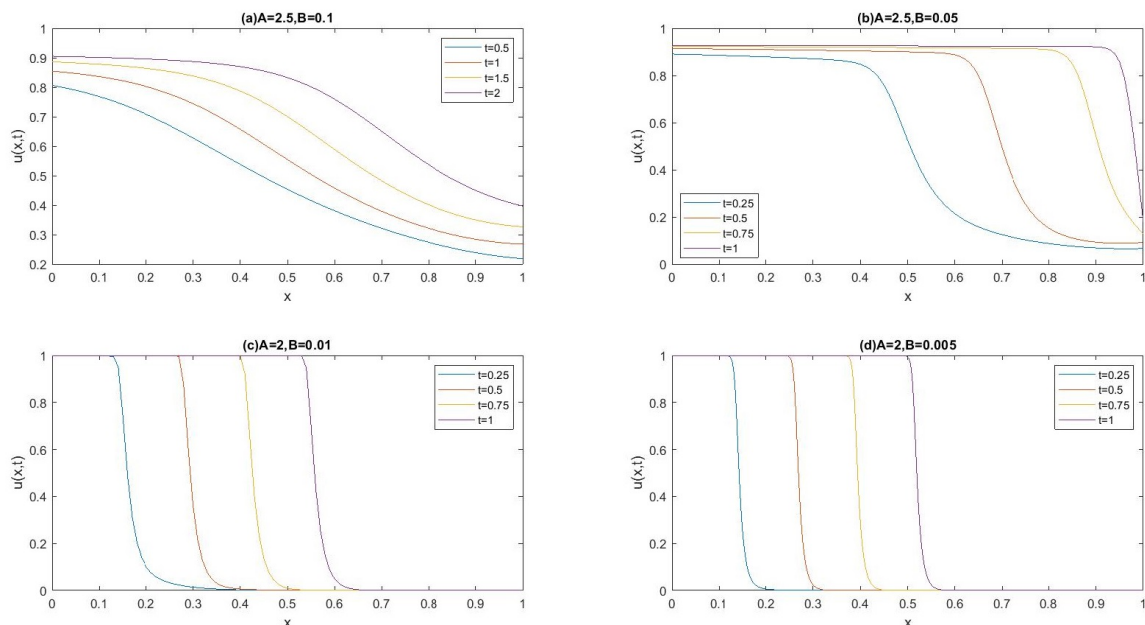


Figure 4. The numerical solution at various time stages using different values for A and B .

Figure 4 demonstrates that the wave propagation accelerates as the dissipation coefficient decreases. Furthermore, the figure also illustrates that as the value of the dissipative coefficient decreases, the wave front tends to exhibit a sharper steepness. In other words, with lower values of the dissipation coefficient, the wave profile becomes more pronounced and intense, indicating a stronger and more distinct wavefront. Figure 4 provides a visual representation of the behavior of shock wave profiles at different time intervals, while considering various values of the dissipation coefficient.

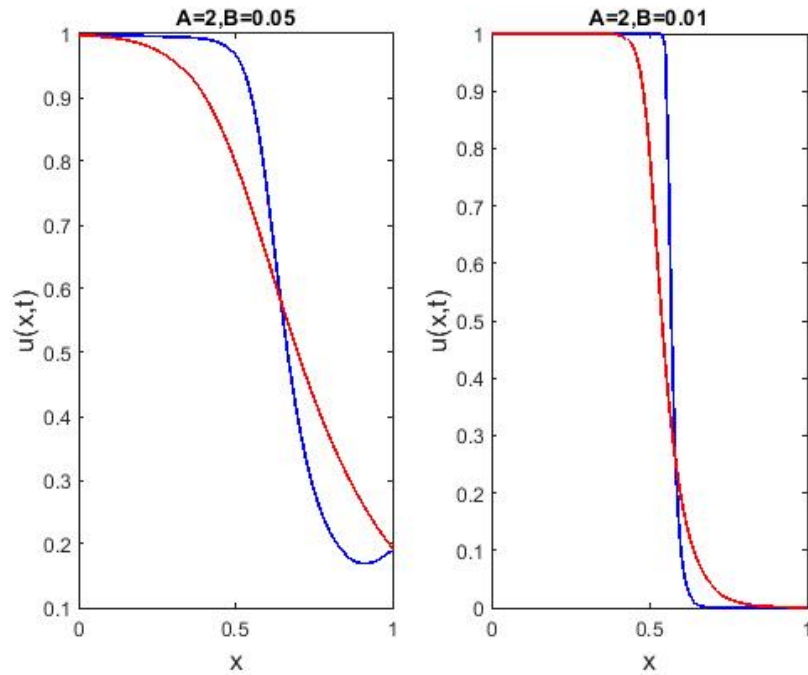


Figure 5. The numerical and analytical solution for various values of A and B (red - analytical, blue - numerical)

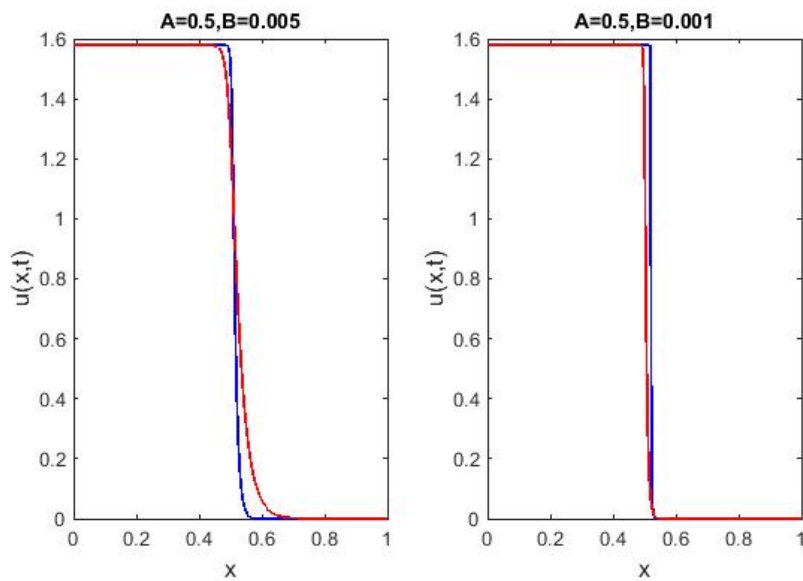


Figure 6. The numerical and analytical solution for various values of A and B (red - analytical, blue - numerical)



Figure 5 and 6 present a comparison between the numerical and analytical solutions at different time points, considering various values of A and B. Upon examination, it can be observed that the graphs representing the

numerical results closely align with the analytical results, particularly when B takes on the values of 0.005 and 0.001.

6. CONCLUSION

In this research, we numerically solve the one-dimensional modified Burgers' equation in dusty plasmas, considering the presence of non-thermal ions with different temperatures. The explicit finite difference technique is employed to solve the equation and investigate the characteristics of shock wave profiles. To assess the accuracy of our approach, we compare the numerical results with analytical results and find that the numerical graphs closely match the analytical ones. Moreover, our numerical solutions outperform those obtained by other methods described in the literature. The results indicate that the accuracy and efficiency of the technique depend on the value of the dissipation coefficient. Specifically, smaller values of the dissipation coefficient yield better results. The research also explores the behavior of shock wave propagation for varying values of the nonlinear coefficient and dissipation coefficient. It is observed that as the dissipation coefficient decreases, the wave front becomes sharper. To assess the accuracy and efficiency of the proposed technique, the absolute error is calculated. The findings indicate that the technique's accuracy and efficiency depend on the value of the dissipation coefficient, with improved results obtained when the dissipation coefficient is smaller.

ORCID

 Harekrishna Deka, <https://orcid.org/0000-0003-4280-3728>;  Jnanjyoti Sarma, <https://orcid.org/0000-0002-0793-5680>

REFERENCES

- [1] S. Raut, K.K. Mondal, P. Chatterjee, and A. Roy, "Propagation of dust-ion-acoustic solitary waves for damped modified Kadomtsev–Petviashvili–Burgers equation in dusty plasma with a q -nonextensive nonthermal electron velocity distribution," *SeMA Journal*, **78**, 571-593 (2021). <https://doi.org/10.1007/s40324-021-00242-5>
- [2] C. Goertz, "Dusty plasmas in the solar system," *Reviews of Geophysics*, **27**(2), 271–292 (1989). <https://doi.org/10.1029/RG027i002p00271>.
- [3] D.A. Mendis, and M.Rosenberg, "Cosmic Dusty Plasma," *Annual Review of Astronomy and Astrophysics*, **32**(1), 419-463 (1994). <https://doi.org/10.1146/annurev.aa.32.090194.002223>.
- [4] P.K. Shukla, "A survey of dusty plasma physics," *Physics of Plasmas*, **8**(5), 1791–1803 (2001). <https://doi.org/10.1063/1.1343087>.
- [5] M. Horányi, and D.A. Mendis, "The dynamics of charged dust in the tail of comet Giacobini Zinner," *Journal of Geophysical Research: Space Physics*, **91**(A1), 355-361 (1986). <https://doi.org/10.1029/SP027p0313>.
- [6] M. Horányi, "Charged dust dynamics in the solar system," *Annual review of astronomy and astrophysics*, **34**(1), 383-418 (1996). <https://doi.org/10.1146/annurev.astro.34.1.383>.
- [7] P.K. Shukla, and L. Stenflo, "Stimulated scattering of electromagnetic waves in dusty plasmas," *Astrophysics and space science*, **190**(1), 23-32 (1992). <https://doi.org/10.1063/1.871450>.
- [8] J. Tamang, and A. Saha, "Phase plane analysis of the dust-acoustic waves for the Burgers equation in a strongly coupled dusty plasma," *Indian Journal of Physics*, **95**(4), 749-757 (2021). <https://DOI:10.1007/s12648-020-01733-3>.
- [9] A. Barkan, A.N. D'angelo, and R.L. Merlino, "Experiments on ion-acoustic waves in dusty plasmas," *Planetary and Space Science*, **44**(1), 239-242 (1996). [https://doi.org/10.1016/0032-0633\(95\)00109-3](https://doi.org/10.1016/0032-0633(95)00109-3).
- [10] P.K. Shukla, and V.P.Silin, "Dust ion-acoustic wave," *Physica Scripta*, **45**(5), 508 (1992). [DOI10.1088/0031-8949/45/5/015](https://doi.org/10.1088/0031-8949/45/5/015).
- [11] R. Merlino, "Dusty plasmas: From Saturn's rings to semiconductor processing devices," *Advances in Physics: X*, **6**(1), 1873859 (2021). <https://doi.org/10.1080/23746149.2021.1873859>.
- [12] S. Ratynskaia, A. Bortolon, and S.I. Krasheninnikov, "Dust and powder in fusion plasmas: Recent developments in theory, modeling, and experiments," *Reviews of Modern Plasma Physics*, **6**(1), 20 (2022). <https://doi.org/10.1007/s41614-022-00081-5>.
- [13] J. Tamang, and A. Saha, "Influence of dust-neutral collisional frequency and nonextensivity on dynamic motion of dust-acoustic waves," *Waves in Random and Complex Media*, **31**(4), 597-617 (2021). <https://doi.org/10.1080/17455030.2019.1605230>.
- [14] A.N. Dev, J. Sarma, and M.K. Deka, "Dust acoustic shock waves in arbitrarily charged dusty plasma with low and high temperature non-thermal ions," *Canadian Journal of Physics*, **93**(10), 1030-1038 (2015). <https://doi.org/10.1139/cjp-2014-0391>.
- [15] R. Tian, L. Fu, Y. Ren, and H. Yang, "(3+1)-Dimensional time-fractional modified Burgers equation for dust ion-acoustic waves as well as its exact and numerical solutions," *Mathematical Methods in the Applied Sciences*, **44**(10), 8177-8196 (2021). <https://doi.org/10.1002/mma.5823>.

- [16] U. Yusuf, M. Yağmurlu, and A. Bashan, "Numerical solutions and stability analysis of modified Burgers equation via modified cubic B-spline differential quadrature methods," *Sigma Journal of Engineering and Natural Sciences*, **37**(1), 129-142 (2019). <https://sigma.yildiz.edu.tr/storage/upload/pdfs/1635837147-en.pdf>
- [17] O. Oruç, "Two meshless methods based on pseudo spectral delta-shaped basis functions and barycentric rational interpolation for numerical solution of modified Burgers equation." *International Journal of Computer Mathematics*, **98**(3), 461-479 (2021). <https://doi.org/10.1080/00207160.2020.1755432>.
- [18] A. Zeytinoglu, M. Sari, and B. Allahverdiev, "Numerical simulations of shock wave propagating by a hybrid approximation based on high-order finite difference schemes," *Acta Physica Polonica A*, **133**(1), 140-151 (2018). <https://doi.org/10.12693/aphyspola.133.140>.
- [19] A.G. Bratsos, "A fourth-order numerical scheme for solving the modified Burgers' equation," *Computers and Mathematics with Applications*, **60**(5), 1393-1400 (2010). <https://doi.org/10.1016/j.camwa.2010.06.021>.
- [20] M.A. Ramadan, T.S. El-Danaf, and F.E. Abd Alaal, "A numerical solution of the Burgers' equation using septic B-splines," *Chaos, Solitons and Fractals*, **26**(4), 1249-1258 (2005). <https://doi.org/10.1016/j.chaos.2005.01.054>.
- [21] D. Irk, "Sextic B spline collocation method for the modified Burgers' equation," *Kybernetes*, **38**(9), 1599-1620 (2009). <https://doi.org/10.1108/03684920910991568>.
- [22] B. Saka, and I. Dag, "A numerical study of the Burgers' equation," *Journal of the Franklin Institute*, **345**(4), 328-348 (2008). <https://doi.org/10.1016/j.jfranklin.2007.10.004>.
- [23] Y. Duan, R. Liu, and Y. Jiang, "Lattice Boltzmann model for the modified Burgers' equation," *Applied Mathematics and Computation*, **202**(2), 489-497 (2008). <https://doi.org/10.1016/j.amc.2008.01.020>
- [24] R.S. Tamsah, "Numerical solutions for convection-diffusion equation using El-Gendi method," *Communications in Nonlinear Science and Numerical Simulation*, **14**(3), 760-769 (2009). <https://doi.org/10.1016/j.cnsns.2007.11.004>
- [25] T. Roshan, and K.S. Bhamra, "Numerical solutions of the modified Burgers' equation by Petrov-Galerkin method," *Applied Mathematics and Computation*, **218**(7), 3673-3679 (2011). <https://doi.org/10.1016/j.amc.2011.09.010>
- [26] S. Kutluay, Y. Ucar, and N.M. Yagmurlu, "Numerical solutions of the modified Burgers' equation by a cubic B-spline collocation method," *Bulletin of the Malaysian Mathematical Sciences Society*, **39**(4), 1603-1614 (2016). <https://doi.org/10.1016/j.amc.2012.01.059>
- [27] Y. Ucar, N.M. Yagmurlu, and O. Tasbozan, "Numerical solutions of the modified Burgers' equation by finite difference methods," *Journal of applied mathematics, statistics and informatics*, **13**(1), 19-30 (2017). <https://doi.org/10.1515/jamsi-2017-0002>
- [28] W. Gao, Y. Liu, B. Cao, and H. Li, "A High-Order NVD/TVD-Based Polynomial Upwind Scheme for the Modified Burgers' Equations," *Advances in Applied Mathematics and Mechanics*, **4**(5), 617-635 (2012). <https://doi.org/10.4208/aamm.10-m1139>
- [29] A. Griewank, and T.S. El-Danaf, "Efficient accurate numerical treatment of the modified Burgers' equation," *Applicable Analysis*, **88**(1), 75-87 (2009). <https://doi.org/10.1080/00036810802556787>
- [30] A.G. Bratsos, and L.A. Petrakis, "An explicit numerical scheme for the modified Burgers' equation," *International Journal for Numerical Methods in Biomedical Engineering*, **27**(2), 232-237 (2011). <https://doi.org/10.1002/cnm.1294>
- [31] Shallu, and V.K. Kukreja, "An improvised collocation algorithm with specific end conditions for solving modified Burgers equation," *Numerical Methods for Partial Differential Equations*, **37**(1), 874-896 (2021). <https://doi.org/10.1002/num.22557>
- [32] A. Kumari, and V.K. Kukreja, "Error bounds for septic Hermite interpolation and its implementation to study modified Burgers' equation," *Numerical Algorithms*, **89**(4), 1799-1821 (2022). <https://doi.org/10.1007/s11075-021-01173-y>
- [33] L. Chandrasekharan Nair, and A. Awasthi, "Quintic trigonometric spline based numerical scheme for nonlinear modified Burgers' equation," *Numerical Methods for Partial Differential Equations*, **35**(3), 1269-1289 (2019). <https://doi.org/10.1002/num.22349>
- [34] G.W. Recktenwald, "Finite-difference approximations to the heat equation," *Mechanical Engineering*, **10** (01) (2004). <https://webspaces.science.uu.nl/~zegel101/MOLMODWISK/FDheat2.pdf>
- [35] M.R. Jana, A. Sen, and P.K. Kaw, "Collective effects due to charge-fluctuation dynamics in a dusty plasma," *Physical review E*, **48**(5), 3930 (1993). <https://doi.org/10.1103/PhysRevE.48.3930>
- [36] J.R. Bhatt, and B.P. Pandey, "Self-consistent charge dynamics and collective modes in a dusty plasma," *Phys. Rev. E*, **50**(5), 3980-3983 (1994). <https://doi.org/10.1103/PhysRevE.50.3980>
- [37] N. Parumasur, R.A. Adetona, and P. Singh, "Efficient solution of burgers', modified burgers' and KdV-burgers'," *Mathematics*, **11**(8), 1847 (2023). <https://doi.org/10.3390/math11081847>

**ЧИСЕЛЬНЕ МОДЕЛЮВАННЯ ТА АНАЛІЗ МОДИФІКОВАНОГО РІВНЯННЯ
БЮРГЕРСА В ЗАПОРОШЕНІЙ ПЛАЗМІ****Харекрішна Дека^a, Джнандйоті Сарма^b**^a Державний відкритий університет К.К. Хандікі, Хананара, Гувахаті, 781022, Індія^b Коледж Р.Г. Баруа, Фатасил Амбарі, Гувахаті, 781025, Індія

У цьому документі представлено всебічне дослідження чисельного моделювання одновимірного модифікованого рівняння Бюргерса в запорошеній плазмі. Для виведення рівняння використовується метод відновних збурень, а числове рішення отримано за допомогою явного методу кінцевих різниць. Отримані результати детально порівнюються з аналітичними рішеннями, демонструючи високий рівень узгодженості, особливо для менших значень коефіцієнта дисипації. Точність і ефективність методики оцінюються за абсолютною похибкою. Крім того, точність і ефективність методики оцінюються шляхом побудови графіків похибок L_2 і L_∞ . Надійність методики додатково підтверджується аналізом стабільності за фон-Нейманом, який вказує на те, що методика умовно стабільна. Загалом дослідження робить висновок, що запропонована методика є успішною та надійною для чисельного моделювання модифікованого рівняння Бюргерса в запиленій плазмі.

Ключові слова: *пилорова плазма; редуکتивний метод збурень; модифіковане рівняння Бюргерса; метод скінченної різниці в явному вигляді; аналіз стійкості фон Неймана*